Biophysical Journal Volume 72 May 1997 2304–2319

The Interaction of Quinone and Detergent with Reaction Centers of Purple Bacteria. I. Slow Quinone Exchange Between Reaction Center Micelles and Pure Detergent Micelles

Vladimir P. Shinkarev and Colin A. Wraight
Department of Plant Biology, Center for Biophysics and Computational Biology, University of Illinois, Urbana, Illinois 61801-3837 USA

ABSTRACT The kinetics of light-induced electron transfer in reaction centers (RCs) from the purple photosynthetic bacterium *Rhodobacter sphaeroides* were studied in the presence of the detergent lauryldimethylamine-*N*-oxide (LDAO). After the light-induced electron transfer from the primary donor (P) to the acceptor quinone complex, the dark re-reduction of P^+ reflects recombination from the reduced acceptor quinones, Q_A^- or Q_B^-. The secondary quinone, Q_B, which is loosely bound to the RC, determines the rate of this process. Electron transfer to Q_B slows down the return of the electron to P^+, giving rise to a slow phase of the recovery kinetics with time $\tau_P \approx 1$ s, whereas charge recombination in RCs lacking Q_B generates a fast phase with time $\tau_{AP} \approx 0.1$ s. The amount of quinone bound to RC micelles can be reduced by increasing the detergent concentration. The characteristic time of the slow component of P^+ dark relaxation, observed at low quinone content per RC micelle (at high detergent concentration), is about 1.2–1.5 s, in sharp contrast to expectations from previous models, according to which the time of the slow component should approach the time of the fast component (about 0.1 s) when the quinone concentration approaches zero. To account for this large discrepancy, a new quantitative approach has been developed to analyze the kinetics of electron transfer in isolated RCs with the following key features: 1) The exchange of quinone between different micelles (RC and detergent micelles) occurs more slowly than electron transfer from Q_B^- to P^+; 2) The exchange of quinone between the detergent "phase" and the Q_B binding site within the same RC micelle is much faster than electron transfer between Q_A^- and P^+; 3) The time of the slow component of P^+ dark relaxation is determined by $\langle n \rangle^{\geq 1}$, the average number of quinones in RC micelles, calculated only for those RC micelles that have at least one quinone per RC (in excess of Q_A). An analytical function is derived that relates the time of the slow component of P^+ relaxation, τ_P, and the relative amplitude of the slow phase. This provides a useful means of determining the true equilibrium constant of electron transfer between Q_A and Q_B (L_{AB}), and the association equilibrium constant of quinone binding at the Q_B site (K_Q^+). We found that $L_{AB} = 22 \pm 3$ and $K_Q = 0.6 \pm 0.2$ at pH 7.5. The analysis shows that saturation of the Q_B binding site in detergent-solubilized RCs is difficult to achieve with hydrophobic quinones. This has important implications for the interpretation of apparent dependencies of Q_B function on environmental parameters (e.g. pH) and on mutational alterations. The model accounts for the effects of detergent and quinone concentration on electron transfer in the acceptor quinone complex, and the conclusions are of general significance for the study of quinone-binding membrane proteins in detergent solutions.

GLOSSARY

k_{AP} rate constant of back reaction between Q_A^- and P^+

$k_p(n)$ rate constant of P^+ dark relaxation in RC micelle with n quinones

$\bar{k}$ second-order rate constant for transfer of quinone from a detergent micelle to a RC micelle (Eq. 22)

k_{-2} rate constant for back-transfer of quinone from RC micelle to detergent micelles (Eq. A9)

k_-^{app} the apparent backward rate constant for the transition from $k + 1$ to k quinone molecules in a RC micelle (Eq. A10)

$K_1 = K_1'[Q]_{det}$ equilibrium constant for partitioning of the first quinone in a RC micelle (Eq. 23)

$K_2 = K_2'[Q]_{det}$ equilibrium constant for partitioning the second and subsequent quinones in a RC micelle (Eq. 23)

K_Q generalized equilibrium constant for quinone binding at the Q_B site (Eq. 3)

K_Q^+ dimensionless intramicellar association constant for quinone binding at the Q_B site

$K_Q(n)$ dimensionless equilibrium constant for quinone binding in a RC micelle with n quinones

L_{AB} equilibrium constant for one electron transfer between Q_A and Q_B

$L_{AB}^{app} = L_{AB}K_Q/(1 + K_Q)$ apparent equilibrium constant for one electron transfer between Q_A and Q_B

$L_{AB}^{app}(n)$ apparent equilibrium constant for one electron transfer between Q_A and Q_B in a RC micelle with n quinones

n number of quinone molecules in a RC detergent micelle

Received for publication 12 August 1996 and in final form 30 January 1997.

Address reprint requests to Dr. Colin A. Wraight, Department of Plant Biology, University of Illinois, 190 ERML/MC-051, 1201 W. Gregory Dr., Urbana, IL 61801-3838. Tel.: 217-333-3245; Fax: 217-244-1336; E-mail: cwraight@uiuc.edu.

0006-3495/97/05/2304/16 $2.00

$\langle n \rangle = n_Q^{RC}/n_{RC}$ average number of quinones per RC micelle (also equal to $[Q]_{RC}/[RC]$)

$\langle n \rangle^{\geq 1}$ average quinone content of RC-detergent micelles exhibiting the slow component of P^+ dark relaxation

P870 or P bacteriochlorophyll dimer in the RC

p_0 probability (fraction) that RC micelle has zero quinone

p_i probability (fraction) of RC micelles with i quinones

Q_A, Q_B the primary and secondary quinone-type electron acceptors in the RC

$[Q]_{det}$ concentration of quinone in detergent micelles, calculated per total volume of the system

$[Q]_{RC}$ concentration of quinone in RC micelles, calculated per total volume of the system

$R = S/(1 - S)$ ratio of the slow and fast components of the P^+ dark relaxation

S fraction of the slow component of the P^+ dark relaxation

α partition coefficient characterizing the vacancy of the Q_B binding site (Eq. A11)

$\rho = K_1/K_2 = 1 + K_Q^+$ constant, characterizing the strength of the quinone binding at the Q_B binding site

τ_{AP} fast time of P^+ dark relaxation, $\tau_{AP} = 1/k_{AP}$

τ_P slow time of P^+ dark relaxation, $\tau_P = 1/k_P$

INTRODUCTION

Photosynthetic reaction centers (RCs) from purple bacteria are one of the best-studied membrane proteins with well-known function. The structures of RCs from two species, *Rhodobacter sphaeroides* and *Rhodopseudomonas viridis*, have been determined precisely by x-ray analysis of crystals (Deisenhofer and Michel, 1989; Allen et al., 1987; El-Kabbani et al., 1991; Ermler et al., 1994; Deisenhofer et al., 1995). The cofactors, bound to the RC, play the role of native reporter groups, allowing sensitive monitoring of structure-function relationships in the RC. These properties, together with their suitability for molecular biology work, make RCs a useful model for other integral membrane proteins.

Of the five essential constituents of isolated RCs—protein, cofactors, detergent (phospholipids), water, and ions—the function and structural organization of the latter three are less well studied because of limited information available from x-ray structural analysis, partly because of their disordering in the crystals. Knowledge of the interactions of all of these components is needed for a proper understanding of the principal mechanisms of RC functioning. The study of the dynamics of detergent interaction with solubilized membrane proteins is also of general importance to our understanding of these systems, and to our ability to use them as models of native membranes.

RCs have been widely studied in the presence of various detergents, of which LDAO (lauryl dimethylamine-*N*-oxide) has been used most frequently (Feher and Okamura, 1978). Even though the RC structure has been determined to atomic resolution, current knowledge concerning the interaction of detergent with RCs is limited, as detergent does not form regular structures in the crystals. By measuring neutron diffraction from reaction center crystals with H_2O/D_2O contrast variation, it was shown that detergent molecules fill the available space around the membrane-spanning α-helices (Roth et al., 1989, 1991). Different estimates give about 200–300 molecules of LDAO bound to the RC (Feher and Okamura, 1978; Gast et al., 1994). This is 3–4 times more than the aggregation number (~75) for pure LDAO detergent micelles (Neugebauer, 1994).

In isolated RCs, after the light-induced electron transfer from the primary donor (P) to the acceptor quinone complex (Q_A and Q_B), the dark reduction of P^+ reflects charge recombination from the reduced acceptor quinones (reviewed in Shinkarev and Wraight, 1993):

$$\begin{array}{ccc} & \overset{k_{BP}}{\downarrow} & \\ P\ Q_AQ_B & \underset{k_{AP}}{\overset{h\nu}{\rightleftharpoons}} & P^+Q_A^-Q_B \underset{k_{BA}}{\overset{k_{AB}}{\rightleftharpoons}} P^+Q_AQ_B^- \end{array} \qquad (1)$$

where k_{AP}, k_{AB}, etc. are rate constants of electron transfer from Q_A^- to P^+, from Q_A^- to Q_B, etc. The direct electron transfer from Q_B^- to P^+ (rate constant k_{BP}) is negligible in wild-type RCs from *Rb. sphaeroides*, and charge recombination from Q_B^- occurs by repopulation of Q_A^- (Kleinfeld et al., 1984a). The direct transfer will be ignored in this work.

The primary quinone, Q_A, is tightly bound and functions as a prosthetic group, but the secondary quinone, Q_B, is readily extracted. When Q_B is absent, the electron transfer $PQ_A \leftarrow P^+Q_A^-$ occurs with a lifetime ($\tau_{AP} = 1/k_{AP}$) of about 0.1 s. When Q_B is present, electron transfer from Q_A^- to Q_B is rapid. Q_B^- is very tightly bound and does not dissociate, even on a time scale of minutes. Transfer of the electron to Q_B slows down the recombination process (re-reduction of P^+) in proportion to the value of the electron transfer equilibrium constant ($L_{AB} = k_{AB}/k_{BA}$):

$$\tau_P = \tau_{AP}(1 + L_{AB}) \qquad (2)$$

where τ_P is the observed time of P^+ re-reduction with functional Q_B, and τ_{AP} is the lifetime of $P^+Q_A^-$ recombination.

This formulation, however, is only valid if the Q_B binding site is fully occupied. In general, the binding of Q_B is not saturated. Within a micelle, or in the native membrane, the residence times for both quinone and quinol (in contrast to the semiquinone) are not more than a millisecond, and the binding equilibrium is established rapidly from the immediate quinone pool, i.e., the membrane in vivo, or from the local micelle environment in isolated, detergent-solubilized RCs. (This is easily deduced from steady-state measurements of RC turnover, which requires binding of quinone and release of quinol, and the known similarity of their binding affinities (Wraight, 1982; Crofts and Wraight, 1983). Under light-limiting conditions, the turnover time of

RCs in detergent suspensions has been reported to be about 1 ms (Rongey et al. 1993), equivalent to a quinone exchange time of 2 ms ($2e^-$ per quinol reduced), and more recent measurements in our laboratory show quinone exchange rates of at least 1 ms^{-1} (J. W. Larson and C. A. Wraight, unpublished observations).) Taking this into account, the charge recombination scheme is modified as follows (Wraight, 1981):

$$\begin{array}{ccc} PQ_AQ_B & \xleftarrow{k_{AP}} & P^+Q_A^-Q_B \xrightarrow{L_{AB}} P^+Q_AQ_B^- \\ \updownarrow K_Q & & \updownarrow \hat{K}_Q \\ PQ_A & \xleftarrow[k_{AP}]{} & P^+Q_A^- \end{array} \quad (3)$$

Here K_Q is the dimensionless equilibrium constant of quinone binding (we assume, for simplicity, that $K_Q = \hat{K}_Q$, i.e., there is no light-induced effect on quinone binding). $K_Q = K'_Q[Q]$, where [Q] is the concentration of free quinone in solution. If the quinone pool is rapidly and homogeneously available to all RCs, the kinetics of P^+ re-reduction are expected to be monophasic, with a lifetime that approaches a limiting slow value as the quinone concentration is raised (reviewed in Shinkarev and Wraight, 1993):

$$\tau_P = \tau_{AP}(1 + L_{AB}^{app}) \quad (4)$$

where

$$L_{AB}^{app} = \frac{L_{AB}K'_Q[Q]}{1 + K'_Q[Q]} \quad (5)$$

The relationships of Eqs. 4 and 5 can be demonstrated under certain circumstances (Wraight and Stein, 1983). However, in isolated RCs, with natural isoprenoid quinones, the kinetics are generally biphasic, with a fast phase arising from RCs lacking Q_B, i.e., $P^+Q_A^-$ recombination, and a slow phase from RCs with Q_B present. Qualitatively, this is readily understandable in terms of a quinone distribution among micelles, with exchange between micelles being slow. Nonetheless, the lifetime of the slow component is still expected to be dependent on the effective quinone concentration in the RC micelle, roughly in accordance with Eqs. 4 and 5. In fact, the nature and behavior of both phases are anomalous. In some detergents, the lifetimes of both phases are quinone concentration dependent, whereas in other detergents neither phase exhibits significant dependence.

Although much characterization of the acceptor quinones has been performed on isolated RCs, the underlying behavior of the quinone binding equilibrium has never been quantitatively accounted for. In this work we examine the dependence of electron transfer on quinone binding, through variation of the LDAO concentration, in *Rb. sphaeroides* RCs. The characteristic time of the slow component of P^+ dark relaxation, observed at low quinone content per RC micelle (at high detergent concentration), is about 1.2–1.5 s, in marked contrast to expectations from the model (see Eqs. 4 and 5), according to which the time of the slow component should approach the time of the fast component (about 0.1 s) when [Q] $\rightarrow$ 0. To account for this discrepancy, as well as other aspects of isolated RC behavior, a new quantitative approach to analyzing the kinetics of electron transfer in detergent-solubilized RCs has been developed, which takes into account known aspects of the RC-quinone binding equilibrium and quinone partitioning into hydrophobic phases. The analysis is in good correspondence with a previous model (Wraight and Stein, 1983) for high quinone concentration, but differs from it significantly for low quinone concentrations. The analytical expressions derived here are applicable to the experimental methodology of flash-induced, single turnovers, but the conclusions are of wider significance for detergent-solubilized membrane proteins.

MATERIALS AND METHODS

Conditions for the growth of *Rb. sphaeroides* cells (wild type, strain Ga, and R26 mutant), as well as isolation of RCs from French press-disrupted cells, were essentially as described by Maróti and Wraight (1988).

Absorption changes were measured on a home-made single-beam spectrophotometer. RCs as prepared had approximately one secondary quinone per RC and were used with no addition of exogenous quinone. After each addition of detergent, the sample was adapted for 5–10 min before measurement. All measurements were done at 22°C. Deconvolution of the kinetic curves into two, three, and more exponentials was accomplished with the program DISCRETE (Provencher, 1986). Deconvolution of the kinetic curves into two exponential components revealed smooth dependencies of the observed times (of about 1 s and 0.1 s) on variable parameters, such as detergent or quinone concentration. Attempts to deconvolute the experimental curves into three exponential components led to irregular dependencies of the observed times and amplitudes on variable parameters. Therefore we limited the deconvolution of the experimental curves to two exponential components (plus a constant). All calculations were made on the software "GIM" (Dr.Achev Development, Tempe, AZ).

RESULTS

Effect of detergents on P^+ dark relaxation

Fig. 1 shows the kinetics of absorption changes at 430 nm (reflecting changes of P^+) at different LDAO concentrations. The addition of LDAO leads to progressive changes in the kinetics of the dark relaxation of P^+. Deconvolution of the kinetic curves usually revealed two exponential components with times of a few hundred milliseconds (slow component) and ~100 ms (fast component). The relative amplitudes of the two phases were clearly dependent on the LDAO concentration.

Fig. 2 shows the time and relative amplitude of the fast and slow components of the P^+ dark relaxation as a function of LDAO concentration added to the sample. The time of the fast component is almost independent of the LDAO concentration (Fig. 2 *A*). The relative amplitude of the fast component increases significantly as the concentration of LDAO increases (Fig. 2 *B*). The behavior of the time of the slow component at very low LDAO concentrations is novel and somewhat unexpected. We believe it is associated with aggregation of the RCs, and we will address it in a subse-

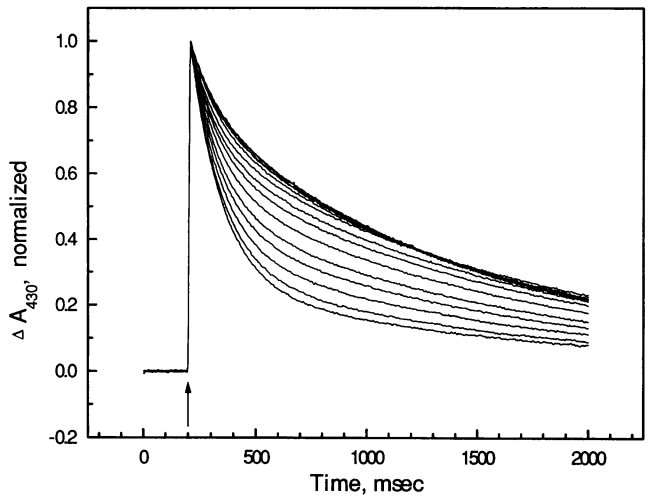

FIGURE 1 Kinetics of the P^+ dark relaxation measured at 430 nm in LDAO-RCs of *Rb. sphaeroides* at different added LDAO concentrations (0, 0.0049, 0.015, 0.03, 0.049, 0.073, 0.12, 0.22, 0.31, 0.47, 0.68, 0.89%), increasing from top to bottom. Incubation medium: 50 mM HEPES, pH 7.5. The concentration of reaction centers was 2.5 μM. No exogenous quinone was added. All curves are normalized to 1 to account for dilution. Even at the highest concentrations of detergent, there was no measurable decrease in signal amplitude beyond the dilution effect.

quent paper. Above ~0.02% LDAO, however, the time of the slow phase is almost constant, decreasing only slightly, whereas the amplitude of the slow phase decreases substantially. This concentration is close to a recent value given for the critical micelle concentration (CMC) for LDAO (Hemelrijk et al., 1995).

The long time of the slow phase (1.2–1.5 s), even at high detergent concentrations, where the quinone is expected to be significantly diluted in the hydrophobic phase of the detergent micelles, is in sharp contrast to simple homogeneous models of the quinone-reaction center interaction (reviewed in Shinkarev and Wraight, 1993), according to which decreasing the quinone concentration should reduce the time of the slow component to that of the fast component (about 0.1 s) as [Q] → 0. This behavior of the dark relaxation of $P870^+$ at low quinone concentrations requires reevaluation of the current descriptions.

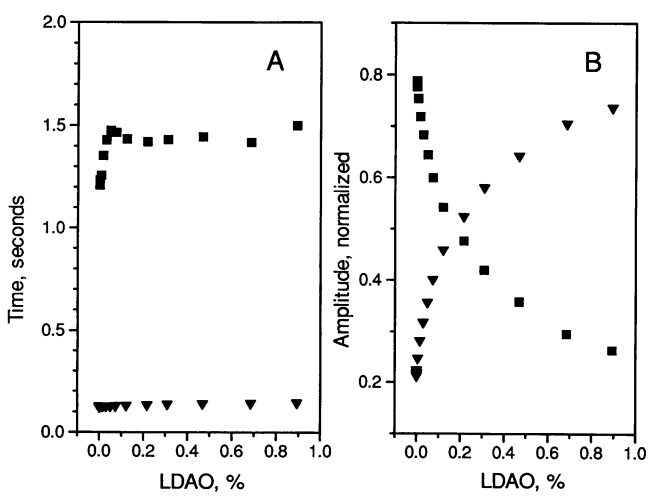

FIGURE 2 (*A*) Dependence of the time (in seconds) of the slow (■) and fast (▼) components of P^+ dark relaxation on LDAO concentration in *Rb. sphaeroides* RCs. (*B*) Dependence of the relative amplitudes of the slow (■) and fast (▼) components of P^+ dark relaxation on LDAO concentration. Conditions are as in Fig. 1.

DISCUSSION

Scheme of reactions. Apparent equilibrium constant of electron transfer between Q_A and Q_B

As a result of exchange of quinones between different micelles, there exist two different types of RC micelles: 1) without quinone (except Q_A); 2) with one or more quinones in excess of Q_A. (All references to "quinone" in this analysis are to secondary or pool quinone, and do not include Q_A, which is presumed to be present in and tightly bound to all RCs.) This is the underlying origin of the biphasic kinetics of P^+ re-reduction. As outlined in the Introduction, however, the kinetics of the slow phase are expected to vary with quinone concentration, in contrast to the observed behavior. To understand the nature of the problem let us assume, first, that the dark relaxation of P^+ occurs faster than redistribution of quinones between RC micelles and detergent micelles. (The term "RC micelle" will be taken to mean a mixed micelle of RC protein and detergent.)

In the microscopic two-phase system, with slow quinone exchange between micelles, the controlling variable for the electron transfer equilibrium is the number, n, of secondary/pool quinone molecules in a RC micelle. Quinone binding at the Q_B binding site of a particular micelle with n quinone molecules can then be described by a scheme similar to Eq. 3:

$$\begin{array}{ccccc} PQ_AQ_B(Q)_{n-1} & \xleftarrow{k_{AP}} & P^+Q_A^-Q_B(Q)_{n-1} & \xleftrightarrow{L_{AB}} & P^+Q_AQ_B^-(Q)_{n-1} \\ \updownarrow K_{Q(n)} & & \updownarrow K_{Q(n)} & & \\ PQ_A(\ldots)(Q)_n & \xleftarrow[k_{AP}]{} & P^+Q_A^-(\ldots)(Q)_n & & \end{array} \qquad (6)$$

where $(Q)_n$ indicates the free quinones (i.e., not bound to the Q_B binding site) within an RC micelle containing a total of n quinones. (. . .) denotes the vacant Q_B binding site. The dimensionless equilibrium constant of quinone binding is assumed to be proportional to the total number of secondary quinones per RC micelle, n (n = 1, 2, 3, etc.):

$$K_Q(n) \equiv \frac{[PQ_AQ_B(Q)_{n-1}]}{[PQ_A(\ldots)(Q)_n]} \approx K_Q^+ \cdot n \qquad (7)$$

K_Q^+ is a (dimensionless) intramicellar association constant for quinone binding. (In a homogeneous solution, the free quinone concentration is established by the average binding

to many RCs:

$$RC + Q \xrightarrow{k_{on}} RCQ_B$$

$$RCQ_B \xrightarrow{k_{off}} RC + Q$$

In a micelle with one RC, it is not. As a first approximation we take the on rate as proportional to n, the total number of quinones present in the RC micelle. Thus the overall binding equilibrium constant, $K_Q(n)$, will also be proportional to n.)

Using Eq. 6, which neglects direct electron transfer from Q_B^- to P^+, and taking into account 1) fast electron exchange between Q_A and Q_B, and 2) fast exchange of quinone between binding site and RC micelle, we can write the following expression for the rate constant of the dark relaxation of P^+ in RC micelles with n quinones:

$$k_p(n) = \frac{k_{AP}(1 + K_Q^+ \cdot n)}{1 + (1 + L_{AB})K_Q^+ \cdot n} = \frac{k_{AP}}{1 + L_{AB}^{app}(n)} \quad (8)$$

where

$$L_{AB}^{app}(n) = \frac{L_{AB}K_Q^+ \cdot n}{1 + K_Q^+ \cdot n} \quad (9)$$

is the apparent equilibrium constant of electron transfer between Q_A and Q_B, which depends on the quinone and detergent content of the RC micelle. (In principle, one can expect K_Q^+ to be dependent on the amount of detergent associated with the RC, and this may account, in part, for the anomalous behavior seen at very low detergent concentrations (Figs. 1 and 2). In the region considered here, however (≥0.02% LDAO), we assume that the detergent-binding capacity of the RCs is saturated.)

Equation 8 can be rewritten for lifetimes ($\tau_P = 1/k_P$, $\tau_{AP} = 1/k_{AP}$) as follows:

$$\tau_P(n) = \tau_{AP}(1 + L_{AB}^{app}(n)) = \tau_{AP}\left(1 + \frac{L_{AB}K_Q^+ \cdot n}{1 + K_Q^+ \cdot n}\right) \quad (10)$$

Kinetics of P^+ dark relaxation

In the limit of slow redistribution of quinones between RC micelles and detergent micelles, the kinetics of P^+ are given by the sum of terms, each of which corresponds to a different number of quinones (0, 1, 2, ...) in the RC micelle:

$$P^+ = p_0 e^{-k_p(0)t} + p_1 e^{-k_p(1)t} + p_2 e^{-k_p(2)t} + \ldots \quad (11)$$

Here $k_p(0)$, $k_p(1)$, etc. are the rate constants of dark reduction of P^+ in RC micelles with zero, one, etc. quinones per RC in excess of Q_A, given by Eq. 8; p_i is the fraction of RC micelles with i quinones. It is evident that the rate constant $k_p(0)$ corresponds to the fast phase of the P^+ dark reduction ($PQ_A \overset{k_{AP}}{\leftarrow} P^+Q_A^-$), whereas rate constants $k_p(1)$, $k_p(2)$, etc. correspond to the slow components of the P^+ dark reduction (Eq. 6).

Equation 11 clearly shows that there is more than one slow component of the P^+ dark relaxation:

$$P^+(\text{slow}) = p_1 e^{-k_p(1)t} + p_2 e^{-k_p(2)t} + \ldots \quad (12)$$

and it follows that a one-exponential approximation for the slow phase of P^+ dark relaxation has sense only when all $k_p(i)$, $i \geq 1$, are close to each other. Current analyses of electron transfer in RCs make the following single-exponential approximation:

$$P^+(\text{slow}) \approx e^{-k_p(\langle n \rangle)t}(p_1 + p_2 + \ldots) \quad (13)$$

where $\langle n \rangle$ is the average number of quinones per RC micelle, $\langle n \rangle = [Q]_{RC}/[RC]$; $[Q]_{RC}$ is the concentration of quinone in RC micelles, calculated per the whole volume of the system, and $k_p(\langle n \rangle)$ is given by (compare with Eqs. 8 and 9)

$$k_p(\langle n \rangle) = \frac{k_{AP}}{1 + L_{AB}^{app}(\langle n \rangle)} \quad (14)$$

where

$$L_{AB}^{app}(\langle n \rangle) = \frac{L_{AP}K_Q^+\langle n \rangle}{1 + K_Q^+\langle n \rangle} \quad (15)$$

(Although Eqs. 8 and 14 look very similar, there is a very big difference between them. Equation 8 is the exact expression for the particular fraction of RCs with n quinones—the whole P^+ decay kinetics would involve a sum of such terms over n. Equation 14 is the one exponential approximation for all fractions, with $\langle n \rangle$ as the average number of quinones (see also Eq. 13 for a definition). A similar comment applies to Eq. 17, except for the use of $\langle n \rangle^{\geq 1}$.) As discussed below, this expression is adequate when the average number of quinones per RC micelle is significantly greater than 1. However, it predicts that k_p approaches the rate constant k_{AP}, as the average number of quinones approaches zero. This conclusion is directly contradicted by experimental observations, as represented by the data in Fig. 2.

Average number of quinones per RC micelle in the fraction that has at least one quinone per RC

To address the contradiction encountered at low quinone concentrations, we must take into account that the slow component of P^+ dark relaxation is observed only in those RCs that have one or more quinones per micelle. Thus we must consider the average number of quinones averaged only over those RC micelles that have at least one quinone:

$$\langle n \rangle^{\geq 1} = \frac{[Q]_{RC}}{[RC]^{\geq 1}} = \frac{[Q]_{RC}/[RC]}{[RC]^{\geq 1}/[RC]} = \frac{\langle n \rangle}{p(\text{at least one quinone})} \quad (16)$$

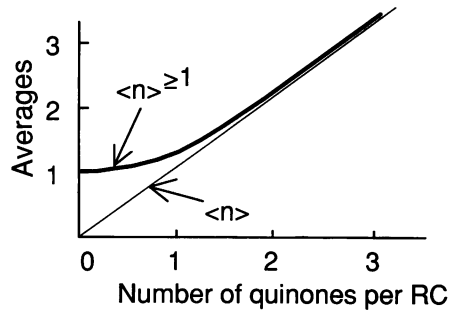

FIGURE 3 Comparison of the average number of quinones per RC micelle, $\langle n \rangle$, and the average number of quinones in those RC micelles that have at least one quinone, $\langle n \rangle^{\geq 1}$.

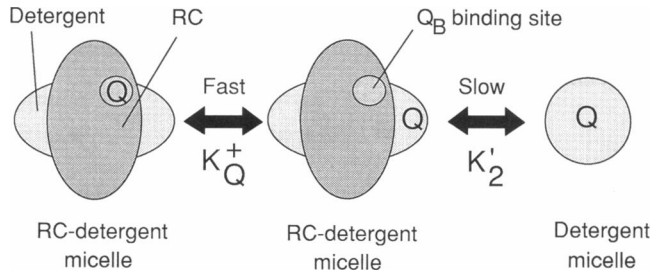

FIGURE 4 Scheme of interaction of quinone with reaction center and with detergent. K_Q^+ is the association equilibrium constant for quinone binding at the Q_B binding site. K'_2 is the equilibrium constant of quinone distribution between the pure detergent micelles and the detergent phase of the RC micelles. See text for details.

here $[RC]^{\geq 1}$ is the concentration of RCs that have at least one secondary/pool quinone, and p(at least one quinone) is the probability (fraction) that a RC micelle has at least one quinone.

Fig. 3 illustrates the relationship between $\langle n \rangle^{\geq 1}$ and $\langle n \rangle$. When the average number of quinones per RC approaches 0, the value of $\langle n \rangle^{\geq 1}$ approaches 1. It is evident from Eq. 16 and from Fig. 3 that $\langle n \rangle^{\geq 1}$ approaches $\langle n \rangle$ at high quinone concentration. Accordingly, we suggest that more appropriate expressions for the rate constant and time of the slow component, in the case of slow exchange of quinone between RC micelles and detergent, are (compare with Eqs. 8 and 14):

$$k_P = \frac{k_{AP}}{1 + L_{AB}^{app}(\langle n \rangle^{\geq 1})} \tag{17}$$

or

$$\tau_P \cong \tau_{AP} \cdot (1 + L_{AB}^{app}(\langle n \rangle^{\geq 1})) \tag{18}$$

where

$$L_{AB}^{app}(\langle n \rangle^{\geq 1}) = \frac{L_{AB} K_Q^+ \cdot \langle n \rangle^{\geq 1}}{1 + K_Q^+ \cdot \langle n \rangle^{\geq 1}} \tag{19}$$

When the average number of quinones per RC micelle, $\langle n \rangle$, approaches zero (and $\langle n \rangle^{\geq 1} \rightarrow 1$), the time of the slow component approaches a limiting value, which can be substantially greater than τ_{AP}:

$$\tau_P \rightarrow \tau_{AP} \cdot \left(1 + \frac{L_{AB} \cdot K_Q^+}{1 + K_Q^+}\right) > \tau_{AP} \tag{20}$$

This clearly corresponds to experiment, in contrast to the traditional approach based on the use of Eq. 14.

Quinone exchange between RC micelles and detergent micelles

To calculate the average number of quinones per RC in those RC micelles having at least one quinone, we must consider a particular model of quinone exchange between RC micelle and detergent (Fig. 4). In the following, the explicit involvement of quinone exchange between RC and detergent micelles defines the resulting model as restricted to conditions where detergent micelles exist (as a reservoir for quinone), i.e., above the CMC. This is widely applicable.

For the present analysis we assume that the time of quinone exchange between different micelles (RC and detergent micelles) is slower than the time of back-reaction between Q_B^- and P^+. Direct measurements have shown this to be approximately true for RCs in LDAO, although the exchange rate may approach or even exceed that of the recombination reaction at elevated temperatures (Wraight and Stein, 1983; McComb et al., 1990). (Fast exchange is described by Eqs. 4 and 5. Analysis of the intermediate exchange case will be considered in a separate paper.)

We also assume that the exchange of quinone between the detergent and the Q_B binding site within the same RC micelle is much faster than electron transfer between Q_A^- and P^+. Fast exchange of quinone within the same RC micelle allows us to use the number of secondary/pool quinones per RC micelle (0, 1, 2, . . .) as a true variable, determined by the intermicelle exchange process:

$$0 \underset{k_{-1}}{\overset{k_1}{\rightleftarrows}} 1 \underset{k_{-2}}{\overset{k_2}{\rightleftarrows}} 2 \underset{k_{-3}}{\overset{k_3}{\rightleftarrows}} \ldots \underset{k_{-n}}{\overset{k_n}{\rightleftarrows}} n \underset{k_{-(n+1)}}{\overset{k_{n+1}}{\rightleftarrows}} \ldots \tag{21}$$

where the numbers 0, 1, 2, . . . n, . . . indicate the number of quinones (in excess of Q_A) per RC micelle.

The following analysis assumes that

1. All forward rate constants k_1, k_2, . . . are simply proportional to the concentration of the quinones in the detergent micelles, constituting a detergent "bulk phase":

$$k_i = \bar{k} \cdot [Q]_{det}$$

2. Backward rate constants of the transitions $i \rightarrow i - 1$ (for $i \geq 2$) are proportional to the number of quinones in the RC micelle, i.e., i (see Appendix):

$$k_{-i} = k'_{-2} \cdot i \quad i \geq 2$$

3. The backward rate constant k_{-1} is different from k'_{-2} because of the binding of quinone at the Q_B binding site (see Appendix):

$$k_{-1} = k'_{-2}/(1 + K_Q^+)$$

The presumption that the backward rate constants (k_{-i}) are proportional to the number of quinones in the RC micelle represents a limiting case of "weak binding" or low occupancy of the Q_B site. The opposite case of strong binding at the Q_B site, where $k_{-i} = k'_{-2} \cdot (i - 1)$, $i \geq 2$, is outlined in the Appendix. As shown below, the situation for LDAO-solubilized RCs lies between these limiting cases, but the weak binding formalism gives good agreement and is simple to handle.

Equation 21 can now be reformulated as (see Appendix)

$$0 \underset{k'_{-2}/(1+K_Q^+)}{\overset{\bar{k}[Q]}{\rightleftharpoons}} 1 \underset{2k'_{-2}}{\overset{\bar{k}[Q]}{\rightleftharpoons}} 2 \underset{3k'_{-2}}{\overset{\bar{k}[Q]}{\rightleftharpoons}} \ldots \underset{nk'_{-2}}{\overset{\bar{k}[Q]}{\rightleftharpoons}} n \underset{(n+1)k'_{-2}}{\overset{\bar{k}[Q]}{\rightleftharpoons}} \ldots \tag{22}$$

The RC micelle transitions of Eq. 22 can also be represented using only equilibrium constants:

$$0 \overset{K_1}{\longleftrightarrow} 1 \overset{K_2/2}{\longleftrightarrow} 2 \overset{K_2/3}{\longleftrightarrow} 3 \ldots \overset{K_2/n}{\longleftrightarrow} n \overset{K_2/(n+1)}{\longleftrightarrow} \ldots \tag{23}$$

Both equilibrium constants, K_1 and K_2, are proportional to the quinone concentration in detergent micelles:

$$K_2 = K'_2[Q]_{det} = \frac{\bar{k}[Q]_{det}}{k'_{-2}}$$
$$K_1 = (1 + K_Q^+)K_2 = \rho K_2 \tag{24}$$

where $\rho = 1 + K_Q^+$.

We can now use Eq. 23 to calculate the average number of quinones per RC ($\langle n \rangle$), as well as the average number of quinones in those RC micelles that have at least one quinone ($\langle n \rangle^{\geq 1}$).

Calculation of $\langle n \rangle$ and $\langle n \rangle^{\geq 1}$ for Eq. 23

As shown in the Appendix, the average number of quinones per RC micelle for Eq. 23 is

$$\langle n \rangle = \frac{\rho K_2 e^{K_2}}{1 + \rho(e^{K_2} - 1)} \approx \begin{cases} \dfrac{\rho K_2(1 + K_2)}{1 + \rho K_2} & K_2 \ll 1 \\ K_2 & K_2 \gg 1 \end{cases} \tag{25}$$

Note that the average number of quinones per RC depends on both K_2 (involving partitioning between RC micelle and detergent) and K_Q^+ (involving equilibrium between the Q_B binding site and the detergent of the same RC micelle). Fig. 5 shows the dependence of the average number of quinones per RC, $\langle n \rangle$, on the equilibrium constant K_2 for different values of K_Q^+.

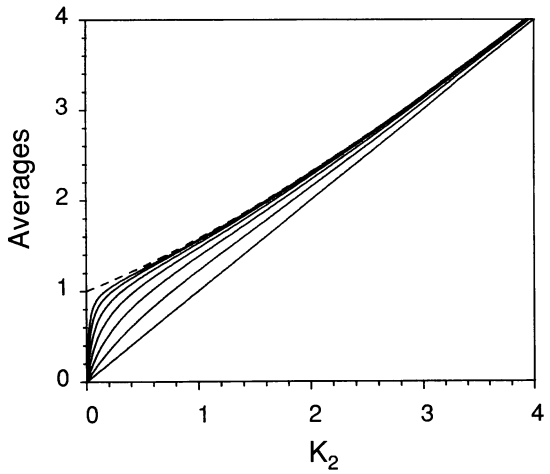

FIGURE 5 Dependence of $\langle n \rangle$, the average number of quinones per RC, on the quinone distribution constant K_2 as a function of the association constant K_Q^+, calculated from Eq. 25. Values of K_Q^+ from bottom to top are 0, 1, 3, 7, 15, 31, 63. The dashed line represents the dependence of $\langle n \rangle^{\geq 1}$, the average number of quinones per RC in those RCs that have at least one quinone, on K_2, calculated from Eq. 26.

The average number of quinones per RC micelle for Eq. 23, calculated for those RC micelles that have at least one quinone per RC, is (see Appendix)

$$\langle n \rangle^{\geq 1} = \frac{K_2}{1 - e^{-K_2}} \tag{26}$$

Fig. 5 (*dashed line*) shows the dependence of $\langle n \rangle^{\geq 1}$ on K_2. Note that $\langle n \rangle^{\geq 1}$ depends only on K_2 and does not depend on K_Q^+. One can see that $\langle n \rangle$ approaches $\langle n \rangle^{\geq 1}$ as the binding constant K_Q^+ is increased. It is also evident from Eqs. 25 and 26 and Fig. 5 that when $K_2 \rightarrow 0$ (e.g., $[Q]_{det} \rightarrow 0$), the average number of quinones per those RC micelles contributing to the slow phase of the P^+ dark reduction, $\langle n \rangle^{\geq 1}$, approaches 1, while the value of $\langle n \rangle$ approaches 0, with a slope depending on the value of K_Q^+.

It is noteworthy that a formally similar expression is obtained on the basis of a Poisson distribution of quinones between different RC micelles, which presumes no specific affinity for quinone at the Q_B binding site and equal distribution between RC micelles and pure detergent micelles (see Appendix):

$$\langle n \rangle^{\geq 1} = \frac{\langle n \rangle}{1 - e^{-\langle n \rangle}} \tag{27}$$

Approximations for the rate constant of P^+ dark relaxation and apparent equilibrium constant L_{AB}^{app}

The similarity of Eqs. 26 and 27, the equivalence of $\langle n \rangle$ and K_2 for large K_2 (Fig. 5, Eq. 25), and the independence of $\langle n \rangle^{\geq 1}$ from K_Q^+ (Eq. 26) lead us to suggest the use of Eq. 27 for estimating $\langle n \rangle^{\geq 1}$ instead of the correct Eq. 26. (This is important from an experimental point of view, as the average number of quinones per RC is easier to measure and to

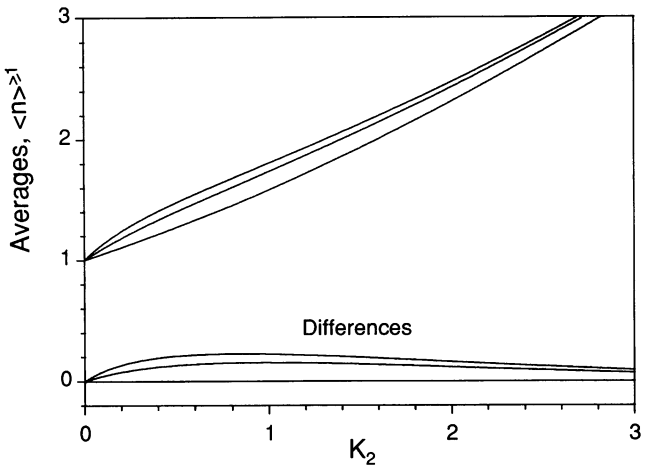

FIGURE 6 Dependence of $\langle n\rangle^{\geq 1}$, the average number of quinones per RC in those RCs that have at least one quinone, on the quinone distribution constant, K_2, as a function of the association constant K_Q^+, calculated from "approximate" Eq. 27, where $\langle n\rangle$ depends on K_2 according to Eq. 25. Values of K_Q^+ from bottom to top are 0, 1, and 2. The curve calculated from Eq. 27 is identical to the curve calculated from "exact" Eq. 26 at $K_Q^+ = 0$ ($\rho = 1$). The differences between the approximate curves and the exact curve are shown at the bottom.

interpret than K_2.) It is also important to note that Eq. 27 predicts the correct behavior of $\langle n\rangle^{\geq 1}$ at both large and small $\langle n\rangle$. It can be seen from Fig. 6 that the deviation of the approximation (given by Eq. 27) from the exact expression (given by Eq. 26) does not exceed 20%, if $K_Q^+ \leq 1$. (Although this limitation for K_Q^+ is not evident a priori, the estimates based on a more general approach, which does not assume that $K_Q^+ \leq 1$, show that $K_Q^+ \approx 0.6 \pm 0.2$ for pH 7.5 (see Fig. 8).)

Thus, if the kinetics of the slow components of dark relaxation of P^+ can be approximated by a single exponent,

$$P^+(\text{slow}) \approx e^{-k_p t}(p_1 + p_2 + \ldots +) \tag{28}$$

the expression for the rate constant k_p can be obtained from Eq. 17 by replacing $\langle n\rangle^{\geq 1}$ by $\langle n\rangle/(1 - e^{-\langle n\rangle})$:

$$k_p = k_{AP}/(1 + L_{AB}^{app}) \tag{29}$$

where

$$L_{AB}^{app} = \frac{L_{AB}K_Q^+\langle n\rangle^{\geq 1}}{1 + K_Q^+\langle n\rangle^{\geq 1}} \approx \frac{L_{AB}K_Q^+\langle n\rangle}{1 - e^{-\langle n\rangle} + K_Q^+\langle n\rangle} \tag{30}$$

For large $\langle n\rangle$ this expression is the same as that used in the traditional approach (Eq. 14), but for $\langle n\rangle < 1$ it differs fundamentally from k_{AP}:

$$\underset{\langle n\rangle \to 0}{k_p} \frac{k_{AP}(1 + K_Q^+)}{1 + (1 + L_{AB})K_Q^+} \tag{31}$$

We stress that all expressions derived here are restricted to the case of slow quinone exchange between RC micelles and pure detergent phase. Furthermore, the approximation of Eq. 30 can only be used if K_Q^+ is relatively small (i.e., weak binding at the Q_B site). Equation 31 is generally valid at low quinone concentrations.

Interdependence of time and amplitude of the slow component of P^+ relaxation for slow exchange of quinone

The time of the slow component of P^+ dark relaxation, τ_P, has been widely used for estimating L_{AB}, whereas the ratio of the slow and fast components of P^+ dark relaxation, $S/(1 - S)$, can be used to characterize the quinone binding at the Q_B binding site in RCs (reviewed in Shinkarev and Wraight, 1993). These are fundamentally linked through the influence of quinone binding on the apparent one-electron transfer equilibrium between Q_A and Q_B (e.g., see Eqs. 9, 19, etc.). Here we show that, for the case of slow exchange of quinones between RC micelles and detergent micelles, the resulting interdependence between the time and amplitude of the slow component of P^+ dark relaxation provides a useful analytical function for determining the true equilibrium constant for one electron transfer (L_{AB}), and the association constant of quinone binding at the Q_B site (K_Q^+).

In RC micelles containing one or more secondary/pool quinones, the kinetics of the dark relaxation of P^+ are slow. The fraction of observed slow component, S, is equal to the probability of finding at least one quinone per RC micelle. (We do not consider the fraction of RCs with a modified Q_B binding site, which is usually in the range of 5–10%.) From Eq. A5 for p_0:

$$S = 1 - p_0 = \frac{\rho(e^{K_2} - 1)}{1 + \rho(e^{K_2} - 1)} \tag{32}$$

As before, K_2 is the equilibrium constant of quinone partitioning into RC micelles and is proportional to $[Q]_{det}$, the concentration of quinone in the detergent phase (see Eq. A3), and $\rho = 1 + K_Q^+$, where K_Q^+ is the equilibrium constant of quinone binding at the Q_B binding site.

Note that if $K_Q^+ = 0$ (i.e., no binding at the Q_B binding site), then $\rho = 1$, $K_2 = \langle n\rangle$ (see Eq. A6), and Eq. 32 reduces to the expression corresponding to a Poisson distribution:

$$S \approx 1 - e^{-K_2} = 1 - e^{-\langle n\rangle} \tag{33}$$

For $K_2 > 0$ the equation for the time of the slow component (see Eqs. 18, 19, and 26) can be written:

$$\tau_P = \tau_{AP} \cdot \left(1 + \frac{L_{AB} \cdot K_Q^+\langle n\rangle^{\geq 1}}{1 + K_Q^+\langle n\rangle^{\geq 1}}\right)$$

$$= \tau_{AP} \cdot \left(1 + \frac{L_{AB} \cdot K_Q^+}{(1 - e^{-K_2})/K_2 + K_Q^+}\right) \tag{34}$$

Both the amplitude (Eq. 32) and the time of the slow component (Eq. 34) depend on the equilibrium distribution constant K_2, which, in general, is not known. However, we can eliminate K_2 from both equations and obtain an expres-

sion describing the dependence of the time of the slow component on the fraction of slow component:

$$\tau_p = f(S; L_{AB}, K_Q^+)$$

This equation contains two parameters: the "true" equilibrium constant of electron transfer between Q_A and Q_B, L_{AB}, and the intramicellar equilibrium binding constant, K_Q^+.

Using the notation $R = S/(1 - S)$ for the ratio of the slow and fast components, we have from Eq. 32

$$K_2 = \ln(1 + R/\rho) \tag{35}$$

$$1 - e^{-K_2} = R/(R + \rho) \tag{36}$$

Inserting Eqs. 35 and 36 into Eq. 34 gives

$$\frac{\tau_P - \tau_{AP}}{\tau_{AP}} = L_{AB}^{app} = \frac{L_{AB} \cdot K_Q^+}{(R/(R + \rho))/\ln(1 + R/\rho) + K_Q^+} \tag{37}$$

(τ_{AP} is usually nearly constant over a wide range of different conditions. Thus the ratio $(\tau_P - \tau_{AP})/\tau_{AP}$ is frequently a function of τ_P only.) This equation describes the relationship between the observed time, τ_P, and the observed fraction of the slow component of P^+ reduction, $S = R/(R + 1)$. The limits of the relationship between τ_P and S are:
For $S \approx 0$ ($R \to 0$),

$$(\tau_P - \tau_{AP})/\tau_{AP} \cdot = \frac{L_{AB} \cdot K_Q^+}{1 + K_Q^+} \tag{38}$$

or

$$\tau_P = \tau_{AP} \cdot \left(1 + \frac{L_{AB} \cdot K_Q^+}{1 + K_Q^+}\right) \tag{39}$$

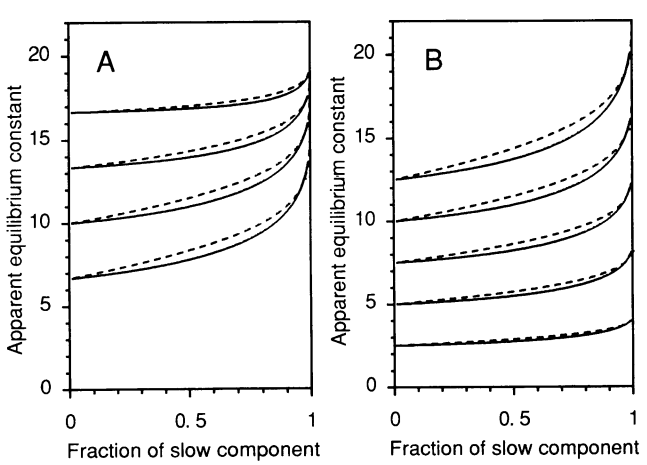

FIGURE 7 Theoretical dependence of $L_{AB}^{app} = (\tau_P - \tau_{AP})/\tau_{AP}$, the apparent equilibrium constant of electron transfer between Q_A and Q_B, on the fraction of the slow component, calculated from Eq. 37, corresponding to the case of weak quinone binding at the Q_B binding site (——), and Eqs. A21 and A22, corresponding to the case of strong quinone binding at the Q_B binding site (– – –). (*A*) Dependence on the quinone binding constant K_Q^+ (with equilibrium constant $L_{AB} = 20$). The values of K_Q^+ from top to bottom are 5, 2, 1, and 0.5, respectively. (*B*) Dependence on equilibrium constant L_{AB} (with quinone binding constant $K_Q^+ = 0.5$). The values of L_{AB} from top to bottom are 25, 20, 15, 10, and 5, respectively.

For $S \approx 1$ ($R \to \infty$),

$$(\tau_P - \tau_{AP})/\tau_{AP} = L_{AB} \tag{40}$$

or

$$\tau_P = \tau_{AP} \cdot (1 + L_{AB}) \tag{41}$$

Fig. 7 shows the theoretical dependence of the apparent equilibrium constant, $L_{AB}^{app} = (\tau_P - \tau_{AP})/\tau_{AP}$ on the fraction of slow component, S, given by Eq. 37 for different L_{AB} and K_Q^+. One can see that L_{AB}^{app} is very sensitive to both K_Q^+ (Fig. 7 *A*) and L_{AB} (Fig. 7 *B*). Note, however, that the relationship between L_{AB}^{app} and S is quite flat over much of the range. Even as S approaches 0, L_{AB}^{app} is significant, reflecting the fact that one quinone in an RC micelle is substantially different from none. As S increases, L_{AB}^{app} responds only weakly until S reaches about 0.8. The final dependence, as S approaches 1 and L_{AB}^{app} approaches its limiting value of L_{AB}, is very steep.

Fig. 8 shows $(\tau_P - \tau_{AP})/\tau_{AP}$ as a function of the fraction of slow component, using experimental data, including those of Fig. 2. The dependence of $(\tau_P - \tau_{AP})/\tau_{AP}$ on S is characterized by two parameters, L_{AB} and K_Q^+. Using nonlinear regression, we determined that $L_{AB} = 22 \pm 3$ and $K_Q^+ = 0.6 \pm 0.2$. The experimentally observed dependence of the apparent equilibrium constant on the fraction of slow-component wild-type *Rb. sphaeroides* RCs is relatively weak. However, the fits are very sensitive to this plateau range of the data (see Fig. 7). Furthermore, the procedure has general significance and can also be used for mutant RCs or RCs from other species, as well as for different detergents under different conditions, such as lower temperature, pH, and salt.

It should be noted that the "true" value of L_{AB} may not be readily apparent from easily achievable values of the slow phase amplitude. Thus, even at $S = 0.8$, indicating 80% of

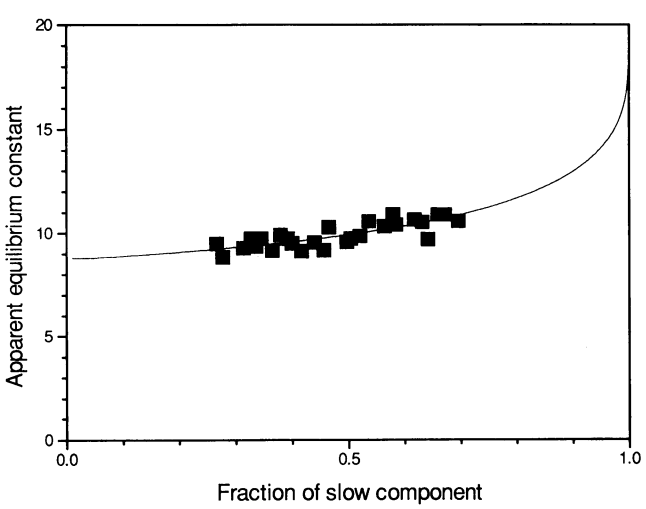

FIGURE 8 Experimental dependence of $(\tau_P - \tau_{AP})/\tau_{AP}$ ($= L_{AB}^{app}$) on the fraction of the slow component of P^+ dark relaxation in *Rb. sphaeroides* RCs, obtained by changing the LDAO concentration. Conditions are as in Fig. 1. The data points are fitted to Eq. 37, with $L_{AB} = 22$ and $K_Q^+ = 0.6$.

the RC micelles have at least one quinone, L_{AB}^{app} is barely half the limiting value of L_{AB}. This is consistent with $K_Q^+ = 0.6$, implying that 1.6 quinones per micelle are required for half-saturation of Q_B binding, whereas a single quinone qualitatively converts the P^+ recombination kinetics from fast to "slow."

Analysis of derived L_{AB} and K_Q^+ values

Our value of $L_{AB} \approx 22$ is 40–60% higher than previously reported values based on the kinetics of $P^+Q_B^-$ charge recombination (Mancino et al., 1984; Kleinfeld et al., 1984a; McComb et al., 1990). However, it is in good agreement with the estimate of Arata and Parson (1981) from the integrated yield of emission of delayed fluorescence from an excited singlet state formed by recombination of $P^+Q_B^-$.

A higher value of L_{AB} for Q-10 as Q_B, is also in very good agreement with those obtained for Q-0, an unprenylated water-soluble analog, when extrapolated to saturating concentrations (McComb et al., 1990; Wraight and Stein, 1983). A lower value for Q-0, reported by Kleinfeld et al. (1984b), was determined at a single, subsaturating concentration. The apparent difference between Q-0 and prenylubiquinones has been discussed in terms of the relative contributions of the quinone headgroup and prenyl tail in establishing binding interactions with the RC protein (McComb et al., 1990; Warncke et al., 1994). It is clear that, because of its water solubility, Q-0 approaches saturation in a simple, hyperbolic fashion (Wraight and Stein, 1983). It now seems that the distribution of hydrophobic prenylquinones in the microscopic two-phase system can depress the measured value of L_{AB} for these compounds.

The good agreement with the value of L_{AB} obtained by Arata and Parson (1981) may arise from the fact that the delayed fluorescence is integrated over the lifetime of the $P^+Q_B^-$ decay, which will minimize the error in the relative contribution of the slow phase kinetics.

The difficulty in achieving saturation at the Q_B binding site, in detergent-solubilized RCs, has important implications for the interpretation of effects imputed to changes in L_{AB}. For example, the pH dependence of the $P^+Q_B^-$ recombination kinetics has been taken to reflect pH dependence of the electron transfer equilibrium constant, L_{AB}. This is only valid as long as the Q_B binding site is saturated, otherwise the pH dependence is indicative only of L_{AB}^{app}. The contributions of L_{AB} and K_Q^+ cannot then be distinguished unless the quinone concentration dependence is measured and taken into account. Similar caveats apply to the interpretation of mutational effects on L_{AB}. In a site-directed mutant of *Rb. sphaeroides* ($Tyr^{L222} \rightarrow Phe$), we have previously reported that the pH dependence of Q_B function is entirely due to changes in K_Q, rather than L_{AB} (Takahashi et al., 1990). Furthermore, when contributions for K_Q and L_{AB} are separated, similar behavior is evident in wild-type RCs for both Q-0 and Q-10 (C. A. Wraight, unpublished observations), casting some doubt on current analyses of the coupled proton and electron transfer processes of the acceptor quinones (reviewed in Okamura and Feher, 1992, 1995; Shinkarev and Wraight, 1993). A strong pH dependence of quinone binding was also reported for RCs of *Chromatium minutissimum* (Shinkarev et al., 1991).

Quinone partitioning between RC and detergent micelles

The model presented here includes two different equilibria involving quinone molecules (see Fig. 4): fast equilibrium between the Q_B binding site and detergent phase inside the RC micelle (equilibrium constant K_Q^+), and slow exchange between RC and detergent micelles (equilibrium constant, K_2'). The derived relationship between τ_P and S (Eq. 37) depends only on K_Q^+, but K_2', and hence the partition coefficient for quinone between the RC and detergent micelles, can also be determined. As a first indication, we note that the value of $K_Q^+ = 0.6$ is equivalent to 1.6 quinones per RC micelle. With about 300 LDAO molecules per RC, this equates to a mole fraction $\approx$ 1/200 (quinone: detergent + quinone). This appears to be substantially weaker binding than that indicated by the quinone content on a total detergent phase basis, e.g., in 0.1% LDAO the dissociation constant for Q-10 binding to the Q_B site is approximately 1/2600 (McComb et al., 1990). However, proper comparison of these values, to yield a partition coefficient for quinone equilibrium between RC and detergent micelles, requires knowledge of the relative micelle concentrations and volumes, and must be based on quantitations of the free quinone concentrations.

K_2' can, in fact, be determined directly from the dependence of the fraction S of the slow component of the P^+ dark relaxation on the quinone concentration. According to Eq. 32 we can write

$$\rho(e^{K_2} - 1) = \frac{S}{1 - S} \tag{42}$$

or

$$K_2 = \ln\left(1 + \frac{S}{\rho(1 - S)}\right) \tag{43}$$

Using the estimated value for $K_Q^+ \approx 0.6$, we have $\rho = 1 + K_Q^+ \approx 1.6$. Hence, at $S = 0.5$,

$$(K_2)_{0.5} = K_2'([Q]_{det})_{0.5} \approx 0.5 \tag{44}$$

When all concentrations are based on the total (aqueous) volume of the sample, the total quinone concentration, $[Q]_{tot}$, is the sum of the quinone concentrations in the detergent phase, $[Q]_{det}$, and in the RC micelles, $[Q]_{RC}$:

$$[Q]_{tot} = [Q]_{det} + [Q]_{RC} = [Q]_{det} + \langle n \rangle [RC] \tag{45}$$

$[Q]_{tot}$ can be estimated from the amplitude of the slow phase at zero added detergent, when all of the quinone is associ-

ated with RC micelles ($[Q]_{tot} = [Q]_{RC}$). From Fig. 2, S = 0.8, meaning that 80% of all RC micelles have at least one quinone. The average quinone content of these RC micelles (see Eq. A6) is

$$\langle n \rangle = \frac{\rho K_2 e^{K_2}}{1 + \rho(e^{K_2} - 1)} \quad (46)$$

At $S = 0.8$, with $\rho = 1.6$, we find from Eq. 43 that $(K_2)_{0.8} = 1.25$. Hence, from Eq. 46, $\langle n \rangle_{0.8} = 1.4$, i.e., 1.4 Q per RC. With [RC] = 2.5 μM, the total quinone concentration is $[Q]_{tot} = 1.4 \times 2.5 = 3.5$ μM. This distribution of quinone is in excellent agreement with the relationship between S and quinone content, determined by extraction and chemical assay (Okamura et al., 1982).

At half-saturation of the slow phase amplitude ($S = 0.5$), half of the RC micelles have at least one quinone. Following the same procedure, we find that $\langle n \rangle_{0.5} = 0.63$. So $([Q]_{RC})_{0.5} = 0.63 \times 2.5 = 1.6$ μM and $([Q]_{det})_{0.5} = [Q]_{tot} - ([Q]_{RC})_{0.5} = 3.5 - 1.6 = 1.9$ μM.

The concentration of free quinone in the RC micelles, $[Q]_{RC}^{free}$, can be determined for Eq. A9, using the approximation of replacing the average of a function by the function of the average ($\Sigma_0 p_k f(k) \approx f(\langle n \rangle)$; see also next section). Hence,

$$[Q]_{RC}^{free} \approx [RC] \cdot \left(\frac{\langle n \rangle}{1 + K_Q^+ \langle n \rangle} + (\langle n \rangle - 1) \frac{K_Q^+ \langle n \rangle}{1 + \langle n \rangle K_Q^+} \right) \quad (47)$$

For $S = 0.5$, $\langle n \rangle_{0.5} \approx 0.63$ and $([Q]_{RC}^{free})_{0.5} \approx 0.9$ μM.

We can now determine the partition coefficient, defined as

$$K_p = \frac{[Q]_{RC}^{free}/[Det]_{RC}}{[Q]_{det}/[Det]_{mic}} = \frac{[Q]_{RC}^{free}[Det]_{mic}}{[Q]_{det} n_{det}^{RC} [RC]} \quad (48)$$

where $[Det]_{RC}$ and [Det] are the concentrations of detergent in RC and detergent micelles, respectively, and $n_{det}^{RC} = 300$ is the number of molecules of detergent per RC micelle (Roth et al., 1989, 1991; Gast et al., 1994, 1996; Hemelrijk et al., 1995). $[Det]_{mic}$ can be obtained from the detergent concentration in excess of the CMC. $S = 0.5$ is reached at an added detergent concentration of 0.17% (see Fig. 2), or 7.4 mM LDAO. With a CMC between 1 and 2 (Hemelrijk et al., 1995), $[Det]_{mic}$ = 5.4–6.4 mM, which we round to 6 mM. With these values in Eq. 49, we can evaluate the partition coefficient, $K_P = 4 \pm 1$. Thus RC micelles adsorb the quinone better than the detergent phase, although not strongly. This may reflect a greater hydrophobicity due, for example, to the nature of the membrane-spanning domain of the RC, or to the greater size of the RC micelle. The LDAO molecule is quite small (12 carbons), and it is easy to imagine that the long (50 carbons) and very hydrophobic isoprene side chain of the quinone is not readily accommodated in a detergent micelle.

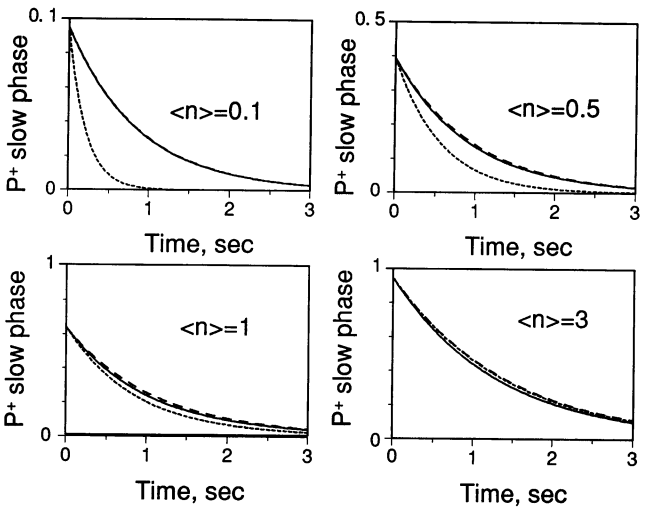

FIGURE 9 Time dependence of the P^+ dark relaxation calculated for three different models as a function of the average number of quinones per RC, $\langle n \rangle$, assuming that $L_{AB} = 20$, $K_Q^+ = 0.6$, $k_{AP} = 10$. ——, "Exact" description of the P^+ dark relaxation as the sum of exponential terms: $P^+(\text{slow}) = p_1 e^{-kp(1)t} + p_2 e^{-kp(2)t} + \ldots + p_8 e^{-kp(8)t}$, where each p_i is calculated from the Poisson distribution: $p_i = (\langle n \rangle^i e^{-\langle n \rangle}/i!)$. Values of $k_P(n)$ are calculated using Eq. 8. – – –, Approximate description of the P^+ dark relaxation as a single exponential on the basis of the "discrete" model proposed here: $P^+(\text{slow}) = e^{-kp(\langle n \rangle^{\geq 1})t}(p_1 + p_2 + \ldots + p_8)$, where each p_i is calculated from the Poisson distribution; $k_P(\langle n \rangle^{\geq 1})$ is given by Eq. 29. ···, Description of the P^+ dark relaxation as a single exponential on the basis of the traditional "continuum" approach: $P^+(\text{slow}) = e^{-kp(\langle n \rangle)t}(p_1 + p_2 + p_8)$, where each p_i is calculated from the Poisson distribution; $k_P(\langle n \rangle)$ is calculated from Eq. 14. Note different ordinate scales at the lower values of $\langle n \rangle$.

Why the traditional approach fails to describe the kinetics of P^+ dark relaxation at low quinone content

The traditional approach, which explicitly or implicitly applies homogeneous kinetics to the description of P^+ dark relaxation, fails drastically at low quinone concentration (see Fig. 9, *dotted line*). The main reason for this is that the real physical system, established by quinone distribution, is discrete, i.e., the number of quinone molecules in a particular RC micelle changes only by integral steps, 0, 1, etc. This cannot by analyzed by continuum methods. Thus the actual quinone content in a particular RC micelle may jump, for example, from 1 to 0, without attaining any intermediate values, but the traditional approach, based on bulk phase quinone concentrations (or average numbers of quinones per RC), assumes that the quinone content in the RC micelle decreases continuously from 1 to 0. The relative error in applying the continuum approach is less the larger the number of quinones per RC, but can be very high if the average number of quinones per RC is close to zero. Experimentally, it is evident that, whereas the average number of quinones per RC can change continuously, the kinetics of P^+ dark relaxation do not. In *Rb. sphaeroides*, the rates of P^+ dark reduction without quinone ($\tau \approx 0.1$ s) and with one quinone ($\tau \approx 1$ s) differ 10-fold. The observed time of the

slow component is determined by the equilibrium constant L_{AB}. In other species or in mutant strains, L_{AB} can be much larger than in wild-type *Rb. sphaeroides*. In such cases, the difference between the traditional (continuum) and new descriptions can be more than two orders of magnitude.

The difference between the new and traditional approaches actually originates in the approximation of the original multiexponential kinetics of the P^+ dark relaxation by a single exponential (see Eqs. 11–13). The problem, then, is how to average a sum of exponential terms. The simplest general method is to replace the average of a function by the function of the average. For any x_i such that $x_i \geq 0$, $\Sigma_{i=0}x_i = 1$, the approximation is

$$\sum_{i=0} x_i f(i) \approx f(\sum x_i i) = f(\langle i \rangle) \tag{49}$$

and this is the approach taken in the traditional analysis (Eq. 13). (The closer the function f is to being linear, the better the approximation.) However, as we have noted, the slow components of the P^+ dark relaxation are observed only in RCs having at least one quinone. Thus the summation of exponential terms in Eq. 11 should begin from $i = 1$. But if the summation begins from $i = 1$ (i.e., $\Sigma_{i=1}q_i = 1$), the approximation of Eq. 49 gives a large error because $x_1 + x_2 + \ldots \neq 1$. This can be overcome by introducing new "weights", $q_i = x_i/(1 - x_0)$, with the same properties as x_i ($q_i \geq 0$, $\Sigma_{i=1}q_i = 1$), as needed for applying Eq. 49:

$$\sum_{i=1} x_i f(i) = (1 - x_0)\sum_{i=1} q_i f(i) \approx (1 - x_0) f\left(\sum_{i=1} q_i i\right)$$

$$= (1 - x_0) f(\langle i \rangle^{\geq 1}) \tag{50}$$

Applying Eq. 50 to the slow components of the P^+ dark relaxation, we have

$$P^+(\text{slow}) = p_1 e^{-k_P(1)t} + p_2 e^{-k_P(2)t} + \ldots +$$

$$\approx (1 - p_0) e^{-k_P(\langle n \rangle^{\geq 1})t} \tag{51}$$

This is exactly the same approximation we used earlier in Eq. 17. A comparison of these approximations is shown in Fig. 9. When the average number of quinones per RC is significant (here $\langle n \rangle = 3$), all approximations are similar. However, for lower quinone concentrations the "continuum" approximation fails drastically. In contrast, the "discrete" approximation is very close to the "exact" (multiexponential) solution for all quinone concentrations.

Note that the total kinetics of the P^+ dark relaxation (including relaxation in RCs without quinone) can be approximated on the basis of Eq. 49:

$$P^+ = p_0 e^{-k_P(0)t} p_1 e^{-k_P(1)t} + p_2 e^{-k_P(2)t} + \ldots + \approx e^{-k_P(\langle n \rangle)t} \tag{52}$$

but it is clearly a poor choice, as long as the rates of the fast and slow phases are very different (here 10-fold), and there is a significant amplitude of the fast phase. In contrast, the one exponential approximation of the slow components is reasonable because the kinetics of the P^+ dark relaxation in RC micelles having 1, 2, and more quinones are relatively close to each other (see dependence of the $k_P(i)$ on i given by the Eq. 8).

CONCLUSIONS

A new quantitative approach has been developed to analyze the kinetics of electron transfer in isolated RCs in the case of slow quinone exchange between different micelles. The main feature of this analysis is the separate consideration of quinone exchange between different micelles (RC and detergent micelles) and the quinone exchange between the detergent "phase" and the Q_B binding site within the same RC micelle. Under these conditions the time of the slow component of P^+ relaxation and the relative amplitude of the slow phase can be related to each other in an explicit fashion. This provides a means of determining the true equilibrium constant of electron transfer between Q_A and Q_B, and the equilibrium constant of quinone binding at the Q_B site. The model accounts for the effects of detergent and quinone concentration on electron transfer in the acceptor quinone complex and can be used to separate the contributions of the true electron transfer and quinone binding equilibrium constants to the observed effects of pH, ionic strength, mutation, etc.

The new model incorporates the traditional model as a special case, and the two give identical results at high quinone concentrations, which, in practice, may be hard to achieve. However, they differ significantly at low quinone concentrations.

The approach described also provides a starting point for a general analysis of the function of detergent-solubilized membrane proteins, where substrate availability may be determined by passive distribution in a detergent phase. Quinone-dependent respiratory and photosynthetic enzymes represent an important and large class of such systems.

APPENDIX I: AVERAGE NUMBER OF QUINONES PER RC, CALCULATED FOR DIFFERENT SCHEMES

Poisson distribution

If quinones are distributed randomly between different RC micelles, the probability of finding a RC micelle with k quinones is given by the Poisson distribution law:

$$p_k = \frac{e^{-\langle n \rangle}\langle n \rangle^k}{k!} \tag{A1}$$

where $\langle n \rangle$ is the average number of quinones per RC micelle. The probability that a RC micelle does not have a quinone ($k = 0$) is $e^{-\langle n \rangle}$, so the probability that at least one quinone is present in a micelle is $1 - e^{-\langle n \rangle}$.

To relate the properties of the slow phase to the prevailing quinone concentration, we must consider the average number of quinones averaged only over those RC-containing micelles with at least one quinone. This is given by

$$\langle n \rangle^{\geq 1} = \frac{\Sigma_{k=1}^{\infty} k p_k}{1 - e^{-\langle n \rangle}} = \frac{\langle n \rangle}{1 - e^{-\langle n \rangle}} \tag{A2}$$

When the average number of quinones per RC micelle is close to zero ($\langle n\rangle \to 0$), the average number of quinones per those RC micelles contributing to the slow phase of the P^+ dark reduction, $\langle n\rangle^{\geq 1}$, approaches 1. When the average number of quinones per micelle is much greater than 1, $\langle n\rangle^{\geq 1}$ approaches $\langle n\rangle$. This relationship is shown in Fig. 3.

Scheme considering the equilibrium between RC and detergent

If the pseudo-first-order rate constant for transfer of quinone out of an RC micelle is proportional to the number of quinone molecules in the RC micelle, we can write the following scheme describing the transitions of a particular RC micelle (see also Eq. 23):

$$0 \underset{K_1}{\longleftrightarrow} 1 \underset{K_2/2}{\longleftrightarrow} 2 \underset{K_2/3}{\longleftrightarrow} 3 \underset{K_2/4}{\longleftrightarrow} 4 \ldots \underset{K_2/n}{\longleftrightarrow} n \qquad \text{(A3)}$$

We assume both K_1 and K_2 to be proportional to the quinone concentration in detergent micelles, e.g. $K_2 = K_2'[Q]_{det}$. Because of the binding of a single quinone by the RC, with intramicelle binding constant K_Q^+, the effective value of the first equilibrium constant (K_1) is significantly different from the others, i.e. $K_1 = (1 + K_Q^+)K_2 = \rho K_2$. We can now find the solution for a finite number of quinones per RC micelle (n), and then obtain simpler (limiting) expressions by extending n to infinity.

For Eq. A3 the probability of finding i quinones in an RC micelle is given by

$$p_i = \frac{K_1 K_2{}^{i-1}/i!}{1 + K_1(1 + K_2/2! + \ldots + K_2{}^{n-1}/n!)} \quad i \geq 1 \qquad \text{(A4)}$$

$$p_0 = \frac{1}{1 + K_1(1 + K_2/2! + \ldots + K_2{}^{n-1}/n!)} \xrightarrow[n\to\infty]{} \frac{K_2}{K_2 + K_1(e^{K_2} - 1)} \qquad \text{(A5)}$$

From Eq. A4, we can calculate the average number of quinones per RC micelle:

$$\langle n\rangle = \sum_k k \cdot p_k = \frac{K_1 \sum_k K_2^{k-1}/(k-1)!}{1 + K_1(1 + K_2/2! + \ldots + K_2^{n-1}/n!)} \xrightarrow[n\to\infty]{} \frac{K_1 K_2 e^{K_2}}{K_2 + K_1(e^{K_2} - 1)} \qquad \text{(A6)}$$

The limits of small and large values of K_2 provide the following two approximations for the average number of quinones per RC micelle:

$$\langle n\rangle \approx \begin{cases} \dfrac{\rho K_2(1 + K_2)}{1 + \rho K_2} & K_2 \ll 1 \\ K_2 & K_2 \gg 1 \end{cases} \qquad \text{(A7)}$$

Thus, at high quinone concentrations, the unknown parameter K_2 is equal to the average number of quinones per RC.

The average number of quinones per RC micelle, calculated only for those that have at least one quinone, is (see Eqs. A5 and A6)

$$\langle n\rangle^{\geq 1} = \frac{\langle n\rangle}{1 - p_0} = \frac{K_2}{1 - e^{-K_2}} \qquad \text{(A8)}$$

$\langle n\rangle^{\geq 1}$ has the following properties (see also Fig. 3):

1. $\langle n\rangle^{\geq 1}$ is independent of the value of K_1 (and, hence, of K_Q^+).
2. When $K_2 \gg 1$, $\langle n\rangle^{\geq 1}$ is just K_2.
3. When $K_2 \ll 1$, $\langle n\rangle^{\geq 1} \approx 1$.

At high quinone concentrations, K_2 is just the average number of quinones (Eq. A7), and the equation for $\langle n\rangle^{\geq 1}$ (Eq. A8) becomes equivalent to the Poisson distribution (Eq. A2).

APPENDIX II: EXPRESSIONS FOR THE EQUILIBRIUM CONSTANTS IN EQ. 23

In the following scheme, the state of the RC micelle is indicated by the ordered pairs: the first number corresponds to the Q_B site occupancy (0 or 1), and the second number corresponds to the number of free quinones in the RC micelle. The rate constants shown are for quinone loss from the RC micelle, i.e., transitions $k \leftarrow (k + 1)$. Not shown are the rate constants for the transitions $k \to k + 1$, because they are all the same ($= \bar{k}[Q]_{det}$) and will not change with the partitioning of quinone between the Q_B binding site and detergent inside the RC micelle:

$$\begin{array}{ccccccc} 0,0 & \xleftarrow{k_{-2}} & 0,1 \ldots 0,k & \xleftarrow{(k+1)k_{-2}} & 0,k+1 & \xleftarrow{(k+2)k_{-2}} & 0,k+2 \ldots \\ & \nwarrow^{K_Q^+} & & \nwarrow^{K_Q^+ k} & & \nwarrow^{K_Q^+(k+1)} & \\ 1,0 \ldots 1,k-1 & \xleftarrow[kk_{-2}]{} & 1,k & \xleftarrow[(k+1)k_{-2}]{} & 1,k+1 \ldots & & \end{array} \qquad \text{(A9)}$$

Assuming that quinone exchange within the RC micelle is faster than quinone exchange between RC micelle and detergent, the apparent backward rate constant for the transition $k \leftarrow (k + 1)$ is the weighted sum of the two possible paths (with and without one quinone bound to the $Q_B$site):

$$k_-^{app} \approx \frac{(k+1)k_{-2}}{1 + (k+1)K_Q^+} + \frac{kk_{-2}(k+1)K_Q^+}{1 + (k+1)K_Q^+} = k_{-2}(k + \alpha_k) \qquad \text{(A10)}$$

where the partition coefficient, α_k, reflects the vacancy of the Q_B binding site:

$$\alpha_k = \frac{1}{1 + (k+1)K_Q^+} \qquad \text{(A11)}$$

(Note that expressions A10 and A11 are also formally valid for $k = 0$, in which case we have $k_-^{app} \approx k_{-2}/(1 + K_Q^+)$.) Thus Eq. A9 can be presented in the following form, reflecting only the total number of quinones in the RC micelle without distinguishing between quinone at the Q_B binding site and free quinones in the RC micelle:

$$k \xleftarrow{(k+\alpha_k)k_{-2}} k+1 \xleftarrow{(k+1+\alpha_{k+1})k_{-2}} k+2 \qquad \text{(A12)}$$

where $0 \leq \alpha_k \leq 1$ for any k. The range of values for α_k provides two distinct limits for k_-^{app}:

$$k_-^{app} \approx \begin{cases} k_{-2}(k+1), & \alpha_k = 1 \text{ (small binding constant } K_Q^+) \\ k_{-2}k, & \alpha_k = 0 \text{ (large binding constant } K_Q^+) \end{cases}$$

Case I: weak binding of quinone at the Q_B binding site (small binding constant, K_Q^+)

In this case $\alpha_k \approx 1$, and the apparent backward rate constant for the transition $k \leftarrow (k + 1)$, $k \geq 1$, is given by

$$k_-^{app} \approx k_{-2}(k+1) \qquad \text{(A13)}$$

Note that in the weak binding case, k_-^{app} corresponds to $k_{-(i+1)}$ in Eq. 21.

Thus the following scheme is a good approximation for the case of weak

quinone binding at the Q_B site (low occupancy):

$$0 \overset{K_1}{\longleftrightarrow} 1 \overset{k[Q]/2k_{-2}}{\longleftrightarrow} 2 \overset{k[Q]/3k_{-2}}{\longleftrightarrow} 3 \ldots \overset{k[Q]/nk_{-2}}{\longleftrightarrow} n \longleftrightarrow \ldots \quad \text{(A14a)}$$

or

$$0 \overset{K_1}{\longleftrightarrow} 1 \overset{K_2/2}{\longleftrightarrow} 2 \overset{K_2/3}{\longleftrightarrow} 3 \ldots \overset{K_2/n}{\longleftrightarrow} n \overset{K_2/(n+1)}{\longleftrightarrow} \ldots \quad \text{(A14b)}$$

The latter scheme is identical to Eq. 23, analyzed in the text.

Case II: strong binding of quinone at the Q_B binding site (large binding constant, K_Q^+)

In this case $\alpha_k \approx 0$, and the apparent backward rate constant for the transition $k \leftarrow (k+1)$ is given by

$$k_-^{app} \approx k_{-2}k \quad \text{(A15)}$$

Incorporating this into a scheme similar to Eq. A14b, involving only the numbers of quinones, gives

$$0 \overset{K_1}{\longleftrightarrow} 1 \overset{K_2}{\longleftrightarrow} 2 \overset{K_2/2}{\longleftrightarrow} 3 \ldots \overset{K_2/(n-1)}{\longleftrightarrow} n \overset{K_2/n}{\longleftrightarrow} \ldots \quad \text{(A16)}$$

Note that the main difference between this scheme and Eq. A14b, corresponding to weak binding, is a shift in number dependence of the expression for the equilibrium constants, i.e., $K_2/k \rightarrow K_2/(k-1)$.

Using Eq. A16, we find the following equations, which provide a full description of RC function at different quinone contents:

$$p_0 = \frac{1}{1 + K_1(1 + K_2 + (K_2^2/2!) + \ldots)} \xrightarrow[n\to\infty]{} \frac{1}{1 + K_1 e^{K_2}}$$

$$= \frac{1}{1 + \rho K_2 e^{K_2}} \quad \text{(A17)}$$

$$1 - p_0 = \frac{K_1 e^{K_2}}{1 + K_1 e^{K_2}} = \frac{\rho K_2 e^{K_2}}{1 + \rho K_2 e^{K_2}} \quad \text{(A18)}$$

$$\langle n \rangle = \sum_k k \cdot p_k \xrightarrow[n\to\infty]{} \frac{K_1(1 + K_2)e^{K_2}}{1 + K_1 e^{K_2}} = \frac{\rho K_2(1 + K_2)e^{K_2}}{1 + \rho K_2 e^{K_2}} \quad \text{(A19)}$$

$$\langle n \rangle^{\geq 1} = \frac{\langle n \rangle}{1 - p_0} = 1 + K_2 \quad \text{(A20)}$$

To find the relationship between time and relative amplitude of the slow component similar to Eq. 37, we can eliminate K_2 by using equations for the apparent equilibrium constant,

$$L_{AB}^{app} = \frac{L_{AB}K_Q^+ \cdot \langle n \rangle^{\geq 1}}{1 + K_Q^+ \cdot \langle n \rangle^{\geq 1}} \approx \frac{L_{AB}K_Q^+ \cdot (1 + K_2)}{1 + K_Q^+ \cdot (1 + K_2)} \quad \text{(A21)}$$

and for the fraction of the slow component,

$$S = 1 - p_0 \approx \frac{\rho K_2 e^{K_2}}{1 + \rho K_2 e^{K_2}} \quad \text{(A22)}$$

TABLE 1 Comparison of strong and weak binding formalisms

Variable of the model	Weak quinone binding approximation, Eq. 23 (considered in the main text) ($\alpha_k \approx 1$ in Eq. A12)*	Strong quinone binding approximation, Eq. A16 (considered in the Appendix) ($\alpha_k \approx 0$ in Eq. A12)
Probability that RC micelle has zero quinone, p_0	$p_0 = \frac{1}{1 + \rho(e^{K_2} - 1)}$ (Eq. A5)	$p_0 = \frac{1}{1 + \rho K_2 e^{K_2}}$ (Eq. A17)
Fraction of the slow component, S	$S \approx \frac{\rho(e^{K_2} - 1)}{1 + \rho(e^{K_2} - 1)}$ (Eq. 32)	$S \approx \frac{\rho K_2 e^{K_2}}{1 + \rho K_2 e^{K_2}}$ (Eq. A22)
Average number of quinones per RC micelle, $\langle n \rangle$	$\langle n \rangle = \frac{\rho K_2 e^{K_2}}{1 + \rho(e^{K_2} - 1)} \underset{K_2\to\infty}{\approx} K_2$ (Eq. A6)	$\langle n \rangle = \frac{\rho K_2 e^{K_2}(1 + K_2)}{1 + \rho K_2 e^{K_2}} \underset{K_2\to\infty}{\approx} K_2$ (Eq. A19)
Average number of quinones per RC micelles exhibiting the slow component of P^+ dark relaxation, $\langle n \rangle^{\geq 1}$	$\langle n \rangle^{\geq 1} = \frac{K_2}{1 - e^{-K_2}}$ (Eq. A8)	$\langle n \rangle^{\geq 1} = 1 + K_2$ (Eq. A20)
Approximation of L_{AB}^{app} using average number of quinones per RC micelle	$L_{AB}^{app} = \frac{L_{AB}K_Q^+\langle n \rangle}{1 - e^{-\langle n \rangle} + K_Q^+\langle n \rangle} \xrightarrow[\langle n \rangle\to 0]{} \frac{L_{AB}K_Q^+}{1 + K_Q^+}$ (Eq. 30)	$L_{AB}^{app} = \frac{L_{AB}K_Q^+(1 + \langle n \rangle)}{1 + K_Q^+(1 + \langle n \rangle)} \xrightarrow[\langle n \rangle\to 0]{} \frac{L_{AB}K_Q^+}{1 + K_Q^+}$ (Eq. A21)
Interdependence between the time and amplitude of the slow component	$\frac{\tau_P - \tau_{AP}}{\tau_{AP}} = \frac{L_{AB} \cdot K_Q^+}{(R/(R + \rho))/\ln(1 + R/\rho) + K_Q^+}$ (Eq. 37)	See Eqs. A21 and A22

*$\alpha_k = 1/(1 + (k + 1)K_Q^+)$, where K_Q^+ is the binding equilibrium constant and k is the number of quinone molecules in the RC micelle. The condition $\alpha_k \approx 1$ is satisfied when $(k + 1)K_Q^+ \ll 1$.

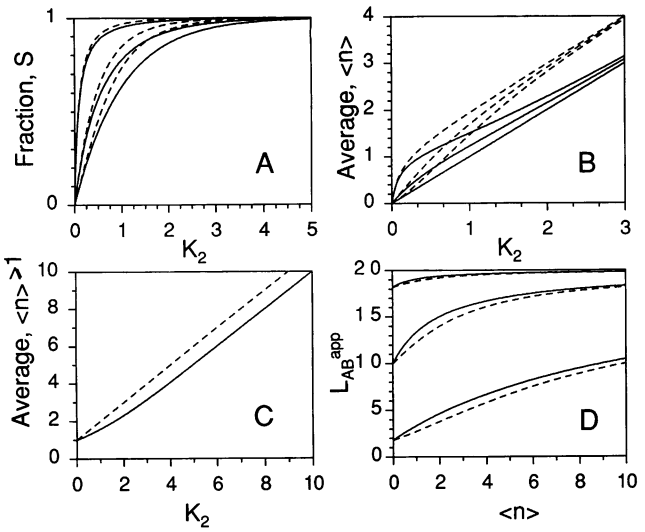

FIGURE 10 Comparison between weak and strong binding models, described by Eqs. 23 and A16, respectively. (*A*) Dependence of the fraction of the slow component on the quinone distribution constant K_2. ——, Weak quinone binding model (Eq. 32); – – –, strong quinone binding model (Eq. A22). Values of K_Q^+ from right to left are 0, 1, and 10. (*B*) Dependence of $\langle n \rangle$, the average number of quinones per RC micelle, on the quinone distribution constant K_2. ——, Weak quinone binding model (Eq. A6); – – –, strong quinone binding model (Eq. A19). Values of K_Q^+ from bottom to top are 0, 1, and 10. At high values of K_Q^+ the two cases tend toward the limiting curves shown in *C*. (*C*) Dependence of $\langle n \rangle^{\geq 1}$, the average number of quinones in RC micelle, having at least one quinone, on the quinone distribution constant K_2. ——, Weak quinone binding model (Eq. A8); – – –, strong quinone binding model (Eq. A20). (*D*) Dependence of the apparent electron transfer equilibrium constant L_{AB}^{app} on the average number of quinones per RC micelle. ——, Weak quinone binding model (Eq. 30); – – –, strong quinone binding model (Eq. A21). Values of K_Q^+ from bottom to top are 0.1, 1, and 10.

This is done by first finding K_2 from Eq. A21 and then plugging it into Eq. A22. The final relationship is large and unwieldy, but can be solved easily by computer.

The results of these calculations for strong and weak binding approximations are summarized in Table 1 and Fig. 10. One can see from Fig. 10 that various characteristics of RCs ($\langle n \rangle$, $\langle n \rangle^{\geq 1}$, L_{AB}^{app}, etc.) are similar for both of these approximations, and their differences do not exceed 20%. Thus each approximation is in reasonable correspondence to the other.

APPENDIX III: COMPARISON OF L_{AB} AND K_Q^+ DETERMINED FROM THE TWO APPROXIMATIONS OF THE MODEL

Interdependence of the time and amplitude of the slow component exists in both approximations of the model (weak and strong quinone binding at the Q_B binding site; see Eqs. 23 and A16). This allows us to determine the applicability of both approximations to LDAO-solubilized reaction centers.

TABLE 2 Analysis of experimental data

	Model used for analysis	
	Weak quinone binding (Eq. 37)	Strong quinone binding (Eqs. A21, A22)
L_{AB}	22 ± 3	30 ± 5
K_Q^+	0.6 ± 0.2	0.35 ± 0.15

TABLE 3 Reciprocal analysis of strong and weak binding models

Model used to create theoretical curve	Model used to determine parameters	L_{AB}	K_Q^+
Weak binding	Weak binding	20	1
Weak binding	Strong binding	17.54 ± 0.02	1.293 ± 0.005
Strong binding	Weak binding	18.03 ± 0.35	1.6 ± 0.1
Strong binding	Strong binding	20	1

Table 2 shows the results found by applying both models to the experimental data of Fig. 8.

Both analyses yield a relatively small value of the quinone binding (association) constant, K_Q^+, indicating that the weak quinone binding model is more appropriate for the description of electron transfer in LDAO RCs.

To further understand how the chosen approximation changes the values determined for L_{AB} and K_Q^+, we took theoretical dependencies derived from the strong and weak binding models with $L_{AB} = 20$ and $K_Q^+ = 1$, and deconvoluted each using both models (Table 3).

The results show that both models give reasonable correspondence within parameters. However, utilization of the inappropriate model for analysis leads to underestimation of L_{AB} and overestimation of K_Q^+. Because the parameter range of interest in this work is close to the limit defining the weak binding approximation ($K_Q^+ \cdot n < 1$), this confirms the appropriateness of the weak binding model for use with the LDAO RC system. Thus in the main text we have focused on this model only.

This work was supported through NSF grants MCB92-08249 and 96-31063 to CAW.

REFERENCES

Allen, J. P., G. Feher, T. O. Yeates, H. Komiya, and D. C. Rees. 1987. Structure of the reaction center from *Rhodobacter sphaeroides* R-26: the protein subunits. *Proc. Natl. Acad. Sci. USA.* 84:6162–6166.

Arata, H., and W. W. Parson. 1981. Delayed fluorescence from *Rhodopseudomonas sphaeroides* reaction centers. Enthalpy and free energy changes accompanying electron transfer from P-870 to quinones. *Biochim. Biophys. Acta.* 638:201–209.

Crofts, A. R., and C. A. Wraight. 1983. The electrochemical domain of photosynthesis. *Biochim. Biophys. Acta.* 726:149–185.

Deisenhofer, J., O. Epp, I. Sinning, and H. Michel. 1995. Crystallographic refinement at 2.3 Å resolution and refined model of the photosynthetic reaction centre from *Rhodopseudomonas viridis*. *J. Mol. Biol.* 246: 429–457.

Deisenhofer, J., and H. Michel. 1989. The photosynthetic reaction centre from the purple bacterium *Rhodopseudomonas viridis*. *EMBO J.* 8:2149–2170.

El-Kabbani, O., C. H. Chang, D. Tiede, J. Norris, and M. Schiffer. 1991. Comparison of reaction centers from *Rhodobacter sphaeroides* and *Rhodopseudomonas viridis*: overall architecture and protein-pigment interactions. *Biochemistry.* 30:5361–5369.

Ermler, U., G. Fritzsch, S. K. Buchanan, and H. Michel. 1994. Structure of the photosynthetic reaction centre from *Rhodobacter sphaeroides* at 2.65 Å resolution: cofactors and protein-cofactor interactions. *Structure.* 2:925–936.

Feher, G., and M. Y. Okamura. 1978. Chemical composition and properties of reaction centers. *In* The Photosynthetic Bacteria. R. K. Clayton and W. R. Sistrom, editors. Plenum Press, New York. 349–386.

Gast, P., P. Hemelrijk, and A. J. Hoff. 1994. Determination of the number of detergent molecules associated with the reaction center protein isolated from the photosynthetic bacterium *Rhodopseudomonas viridis*. Effects of the amphiphilic molecule 1,2,3-heptanetriol. *FEBS Lett.* 337: 39–42.

Gast, P., P. Hemelrijk, H. J. van Gorkom, and A. J. Hoff. 1996. The association of different detergents with the photosynthetic reaction center protein of *Rhodobacter sphaeroides* R26 and the effects on its photochemistry. *Eur. J. Biochem.* 239:805–809.

Hemelrijk, P. W., P. Gast, H. J. van Gorkom, and A. J. Hoff. 1995. The association of different detergents with the photosynthetic reaction centers protein of *Rhodobacter sphaeroides* R26 and the effects on its photochemistry. *In* Photosynthesis: From Light to Biosphere, Vol. 1. P. Mathis, editor. Kluwer Academic Publishers, Dordrecht, The Netherlands. 643–646.

Kleinfeld, D., E. C. Abresch, M. Y. Okamura, and G. Feher. 1984a. Damping of oscillations in the semiquinone absorption in reaction centers after successive flashes. Determination of the equilibrium between $Q_A^- Q_B \rightarrow Q_A Q_B^-$. *Biochim. Biophys. Acta.* 765:406–409.

Kleinfeld, D., M. Y. Okamura, and G. Feher. 1984b. Electron transfer in reaction centers of *Rhodopseudomonas sphaeroides*. I. Determination of the charge recombination pathway of $D^+Q_AQ_B^-$ and free energy and kinetic relations between $Q_A^-Q_B \rightarrow Q_AQ_B^-$. *Biochim. Biophys. Acta.* 766:126–140.

Mancino, L. J., D. P. Dean, and R. E. Blankenship. 1984. Kinetics and thermodynamics of the $P870^+Q_A^- \rightarrow P870^+Q_B^-$ reaction in isolated reaction centers in the photosynthetic bacterium *Rhodopseudomonas sphaeroides. Biochim. Biophys. Acta.* 764:46–54.

Maróti, P., and C. A. Wraight. 1988. Flash-induced H^+ binding by bacterial photosynthetic reaction centers. Influences of the redox states of the acceptor quinones and primary donor. *Biochim. Biophys. Acta.* 934: 329–347.

McComb, J. C., R. R. Stein, and C. A. Wraight. 1990. Investigations on the influence of head-group substitution and isoprene side-chain length in the function of primary and secondary quinones of bacterial reaction centers. *Biochim. Biophys. Acta.* 1015:158–171.

Neugebauer, J. 1994. A Guide to the Properties and Uses of Detergents in Biology and Biochemistry. Calbiochem. Hoechst Celanese Corporation, San Diego, CA.

Okamura, M. Y., R. J. Debus, D. Kleinfeld, and G. Feher. 1982. Quinone binding sites in reaction centers from photosynthetic bacteria. *In* Function of Quinones in Energy Conserving Systems. B. L. Trumpower, editor. Academic Press, New York. 299–317.

Okamura, M. Y., and G. Feher. 1992. Proton transfer in reaction centers from photosynthetic bacteria. *Annu. Rev. Biochem.* 61:861–896.

Provencher, S. W. 1976. A Fourier method for analysis of exponential decay curves. *Biophys. J.* 16:27–41.

Rongey, S. H., M. L. Paddock, G. Feher, and M. Y. Okamura. 1993. Pathway of proton transfer in bacterial reaction centers: second-site mutation Asn-M44→ Asp restores electron and proton transfer in reaction centers from the photosynthetically deficient Asp-L213 → Asn mutant of *Rhodobacter sphaeroides. Proc. Natl. Acad. Sci. USA.* 90: 1325–1329.

Roth, M., B. Arnoux, A. Ducruix, and F. Reiss-Husson. 1991. Structure of the detergent phase and protein-detergent interactions in crystals of the wild-type (strain Y) *Rhodobacter sphaeroides* photochemical reaction center. *Biochemistry.* 30:9403–9413.

Roth, M., A. Lewit-Bentley, H. Michel, J. Deisenhofer, R. Huber, and D. Oesterhelt. 1989. Detergent structure in crystals of a bacterial photosynthetic reaction centre. *Nature.* 340:659–661.

Shinkarev, V. P., M. I. Verkhovsky, J. Sabo, N. I. Zakharova, and A. A. Kononenko. 1991. Properties of photosynthetic reaction centers isolated from chromatophores of *Chromatium minutissimum. Biochim. Biophys. Acta.* 1098:117–126.

Shinkarev, V. P., and C. A. Wraight. 1993. Electron and proton transfer in the acceptor quinone complex of reaction centers of phototrophic bacteria. *In* The Photosynthetic Reaction Center, Vol. 1. J. Deisenhofer and J. R. Norris, editors. Academic Press, San Diego, CA. 193–255.

Takahashi, E., P. Maróti, and C. A. Wraight. 1990. Site-directed mutagenesis of *Rhodobacter sphaeroides* reaction center: the role of tyrosine L222. *In* Current Research in Photosynthesis, Vol. 1. M. Baltschevsky, editor. Kluwer Academic Publishers, Norwell, MA. 169–172.

Warncke, K., M. R. Gunner, B. S. Braun, L. Gu, C.-A. Yu, J. M. Bruce, and P. L. Dutton. 1994. Influence of hydrocarbon tail structure on quinone binding and electron-transfer performance at the Q_A and Q_B sites of the photosynthetic reaction center protein. *Biochemistry.* 33:7830–7841.

Wraight, C. A. 1981. Oxidation-reduction physical chemistry of the acceptor quinone complex in bacterial photosynthetic reaction centers. Evidence for a new model of herbicide activity. *Isr. J. Chem.* 21: 348–354.

Wraight, C. A. 1982. The involvement of stable semiquinone in the two electron gates of plant and bacterial photosynthesis. *In* Function of Quinones in Energy Conserving Systems. B. L. Trumpower, editor. Academic Press, New York. 181–197.

Wraight, C. A., and R. R. Stein. 1983. Bacterial reaction centers as a model for photosystem II: turnover of the secondary acceptor quinone. *In* The Oxygen Evolving System of Photosynthesis. Y. Inoue et al., editors. Academic Press, Tokyo. 383–392.